1986RMxAA..12..273D

Rev. Mexicana Astron. Astrof., **12**, 273-282 (1986

PHOTOELECTRIC PHOTOMETRY OF CED 128 - A REFLECTION NEBULA

M. de Oliveira, W. J. Maciel

Instituto Astronômico e Geofísico
Universidade de São Paulo
Brasil

RESUMO. Neste trabalho são apresentadas curvas observacionais de $(B-V)_{*-neb}$ ao longo de quatro direções radiais à estrela iluminadora, ν Sco. Para reproduzir estes resultados, modelos nebulares plano-paralelos foram combinados com treze materiais prováveis constituintes do meio interestelar. Aplicou-se a teoria exata de Mie para espalhamento por esferas. De acordo com o excesso de cor da estrela (E_{B-V} = 0,28), ν Sco provavelmente encontra-se imersa na nebulosa, cuja espessura seria de aproximadamente 1,5 pc, inclinada a 10^{o} com relação ao plano do céu. Gelo, gelos sujos e silicatos são os materiais que melhor reproduzem as observações ao longo das direções consideradas. Não obstante, magnetita, carbeto de silício e amônia não podem ser descartados.

ABSTRACT. In this work we present $(B-V)_{*-neb}$ curves along four radial directions relative to the illuminating star, ν Sco. Several plane-parallel model nebulae were combined with thirteen grain materials, which are thought to be constituents of the general ISM. The exact Mie theory of scattering by spheres was applied. It is derived that ν Sco is probably embedded in the nebula, and that its thickness is approximately 1,5 pc and the tilting angle is 10^{o}, in good agreement with the expected location suggested by the star's color excess E_{B-V} = 0,28. Ice, dirty ices and silicates give the best general fittings for all directions considered. Magnetite, silicon carbide and NH_3 cannot however be excluded.

Key words: reflection nebulae - photometry - interstellar grains.

© Universidad Nacional Autónoma de México • Provided by the NASA Astrophysics Data System

1986RMxAA..12..273D

I. INTRODUCTION

Basically, reflection nebulae are conglomerates of dust grains that reflect the visible light of a nearby illuminating star, whose spectral type is usually later than B1.

There have been many attempts to infer the optical properties, chemical composition and characteristic sizes of dust particles on the basis of photometric and polarimetric observations and theoretical models of reflection nebulae (Schalén, 1945; Roark, 1966; Hanner, 1969; Zellner, 1970; Shah & Swamy, 1981; King *et al.*, 1983; Sellgren, 1984). Nevertheless, no study has succeeded in determining both the grain properties and nebular geometry unambiguously.

In this work, BV photometric measurements are presented of the reflection nebula Ced 128 along four radial directions relative to the illuminating star, ν Sco ($\alpha_{1900} = 16^h\ 06^m$; $\delta_{1900} = -19^0\ 12'$).

Following the procedure of Hanner (1969), plane-parallel model nebulae were employed with thirteen candidate grain materials, assuming the nebular dust to be similar to that found in the general interstellar medium (hereinafter ISM)

II. OBSERVATIONS

The UBVR photoelectric measurements were carried out at the OAB (Observatório Astrofísico Brasileiro) 1.6 m telescope near Brasópolis, Brasil, during 1981/1982.

The IAG (Instituto Astronômico e Geofísico da USP) double-beam chopping polarimeter, used as a photometer, allowed simultaneous observations of two contiguous nebular regions. This also reduced much of the time spent with calibration and extinction stars through simultaneous measurements of the sky.

The scattered light "halation" effect, after Zellner, 1970) of the nebulosity-free stars HD 130841, HD 148184 and HD 175191 was measured at the same position angles and distances as the observed nebular regions.

The observations were made along the four radial directions: SW, NE, N and S of the illuminating star. The results were expressed as $(B-V)_*-(B-V)_{neb}$ and plotted against the offset angle Φ. The mean dispersion of the points for each direction is shown in Figure 1 and it amounts to 0.3 mag for the SW and NE directions, and 0.1 mag for N and S. The mean internal error amounts to ~ 0.1 mag. Each point is an average of the values obtained for each viewing angle.

All directions exhibit the general trend of being bluer than the star at small offset angles, progressively reddening as Φ increases. A difference in reddening steepness may be expected after an inspection of the ESOSS plates, where one can see the clear-cut edge of the nebula SW of the star. On the other

© Universidad Nacional Autónoma de México • Provided by the NASA Astrophysics Data System

1986RMxAA..12..273D

hand, the object seems to faint gradually along the opposite direction. For the NE, N and S directions, a smooth gradient in color index can be seen. A certain degree of similarity can nevertheless be noticed in the color index values at Φ 0^0 for the different directions.

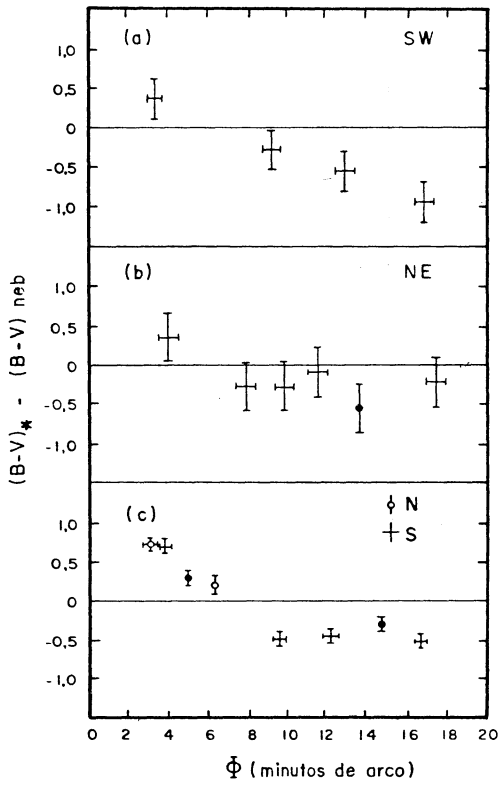

FIGURE 1. Observational data for Ced 128 along four radial directions to ν Sco.

III. MODELS

(a) Nebular Models

A plane-parallel model nebula in the form of an infinite and homogeneous slab of dust with three possible locations for the illuminating star was the basic model employed. The star could be located "behind", "inside" or "in front" of the slab relative to the observer. See Figure 2 for a sketch of the star - in-front geometry.

Single scattering was assumed and treated analytically according to the exact Mie theory for spheres (Mie, 1908; Debye, 1909; van de Hulst, 1957).

The observed nebular surface brightness for a given filter in the observer's system can be expressed as:

© Universidad Nacional Autónoma de México • Provided by the NASA Astrophysics Data System

1986RMxAA..12..273D

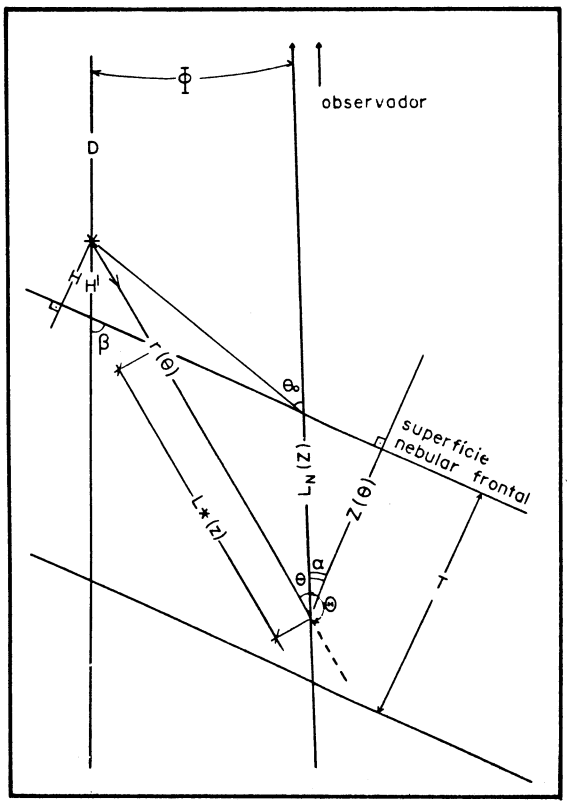

FIGURE 2. Schematic diagram of the star-in-front geometry.

$$I_{neb}(\Delta\lambda,\Phi) = \int_{\lambda_1}^{\lambda_2} d\lambda\, Q(\lambda)\, I_*(\lambda)\, \frac{\gamma^2\lambda^2}{32\,\pi^2}\, \sec\alpha(\Phi)\, d\Omega \int_0^T \frac{dz}{r(z)^2}\, e^{-\kappa(\lambda)\left[L_*(z)-L_{neb}(z)\right]}$$

$$\times \int_{a_1}^{a_0} da\, n(a)\, F(\lambda,a,\theta) \qquad (1)$$

where:

$Q(\lambda)$ is a combination of the transmission functions of the telescope optic photomultiplier, terrestrial atmosphere and intestellar extinction,

$I_*(\lambda)$ is the spectral energy distribution of the illuminating star,

γ is the stellar radius,

$d\Omega$ is the solid angle comprised by the diaphragm,

$\kappa(\lambda)$ is the nebular linear extinction coefficient,

$n(a)$ is the grain size distribution $= n_0\, e^{-5(a/a_0)^3}$

© Universidad Nacional Autónoma de México • Provided by the NASA Astrophysics Data System

1986RMxAA..12..273D

$F(\lambda,a,\Theta)$ is the scattering phase function for a grain of radius a and a scattering angle Θ ,

α is the angle between the line of sight and the normal to the nebular face,

$r(z)$ is the total light path length to the scattering volume element at a depth z ,

$L_*(z)$ is the portion of the trajectory traversed by the light within the nebula before reaching the scattering volume element,

$L_N(z)$ is the analogous portion of the path between the volume and the front nebular boundary.

The adopted distance of the system is D= 172 pc (Hardie & Crawford, 1961). The best models were obtained with $\beta = 100^0$. Both these values are used throughout this paper. The stellar spectral energy distribution was taken from Kurucz (1979) (T_{eff} = 22500 K, log(g)= 3.5), and solar chemical abundance.

If the star is behind the nebula,

$$I_{*_{obs}}(\Delta\lambda) = \int_{\lambda_1}^{\lambda_2} d\lambda\, I_{*_0}(\lambda)\, Q(\lambda)\, e^{-\kappa(\lambda)\, T/\sin\beta} \qquad (2)$$

and for the star-inside case,

$$I_{*_{obs}}(\Delta\lambda) = \int_{\lambda_1}^{\lambda_2} d\lambda\, I_{*_0}(\lambda)\, Q(\lambda)\, e^{-\kappa(\lambda)\, H'} \qquad (3)$$

In order to calibrate to the Jonson's standard system, we adopted the mean values of our transformation coefficients (Hardie, 1962):

$$(B-V) = (1.02 \pm 0.03)\,(b-v)_0 - (0.16 \pm 0.03) \qquad (4)$$

$$V = v_0 - (0.04 \pm 0.02)\,(B-V) + (21.37 \pm 0.01) \qquad (5)$$

The star-minus-nebula differences of color indices follow immediately.

The nebular linear extinction values were taken from Boggess & Borgman (1964), used with A_V= 1.3 mag/pc at λ5540 Å.

(b) Grain Models

The ISM is no longer regarded as a realistic birthplace of interstel-

© Universidad Nacional Autónoma de México • Provided by the NASA Astrophysics Data System

1986RMxAA..12..273D

lar grains. Cool stellar atmospheres and extended envelopes are probably more suitable sites for nucleation. Embryos are possibly composed of refractory materials such as silicates, oxides, graphite and carbides from C stars. They can be further coated with icy or organic materials (Cameron, 1975; Whittet , 1981; Rossi & Maciel, 1984, and references therein).

A total of thirteen materials was selected: ice, two types of dirty ice, olivine, magnetite, obsidian, basalt, silicon, silicon carbide, graphite, iron, NH_3 ice and silica.

The grains were assumed to be spherical, homogeneous and constituted by only one material. The adopted particle size distribution is the Oort-van de Hulst-Greenberg distribution (Oort & van de Hulst, 1946; Greenberg, 1968):

$$n(a) = n_0 \, e^{-5(a/a_0)^3} \qquad (6)$$

The adopted size parameters were: a_0(ice, dirty ices)= 0.5μ; a_0(silicon)= 0.1μ; a_0(obsidian, SiC, olivine, basalt)= 0.2μ; a_0(magnetite, silica)= 0.25μ; a_0(iron, graphite)=0.51μ and $a_0(NH_3)$= 1μ.

IV. COMPARISON WITH OBSERVATIONS

Nearly 200 models combining different geometrical parameters and grain materials were analyzed. A set of ten representative model nebulae was chosen and tested for with every candidate material.

Five general tendencies were noticed:

(1) $\beta = 100^0$ is the most suitable value for this study.

(2) The $(B-V)_\star - (B-V)_{neb}$ curves flatten as the light path length increases.

(3) Iron, silicon and graphite usually produce $(B-V)_\star - (B-V)_{neb}$ curves that are bluer than indicated by the observations. Consequently, these materials were ruled out.

(4) Changes in H affect primarily the regions within 6', altering the maximun values of $(B-V)_\star - (B-V)_{neb}$ up to 0.5 mag.

(5) Values of H $\geq$1 are not suitable because they produce strong deviations from the observed $(B-V)_\star - (B-V)_{neb}$ curves, whatever the model employed.

© Universidad Nacional Autónoma de México • Provided by the NASA Astrophysics Data System

1986RMxAA..12..273D

We tried to reproduce each direction separately, but the results turned out to be quite similar. For that reason, and due to the fact that the observational data do not permit an individual characterization of each direction, the best fits are represented all in the same picture (Figure 3) together with the observational data for all the directions studied.

(a) Star Behind

These models always produced color indices that are much bluer than the star's, no matter what material was employed. Despite the occurrence of negative difference values, ice, dirty ices and magnetite could not reproduce the observed features.

(b) Star in Front

These models depend critically both on the distance H and the back-scatter efficiency (Q_{back}) of the grains. The parameters β and T affect the color indices to a smaller degree. These models are characterized by maxima and minima up to 0.5 mag near the star, followed by a smooth reddening as Φ increases. In addition, as long as H < 0.9 pc, these models exhibit a very blue nebular color index near the star, followed by a reddening whose steepness depends on the actual H value.

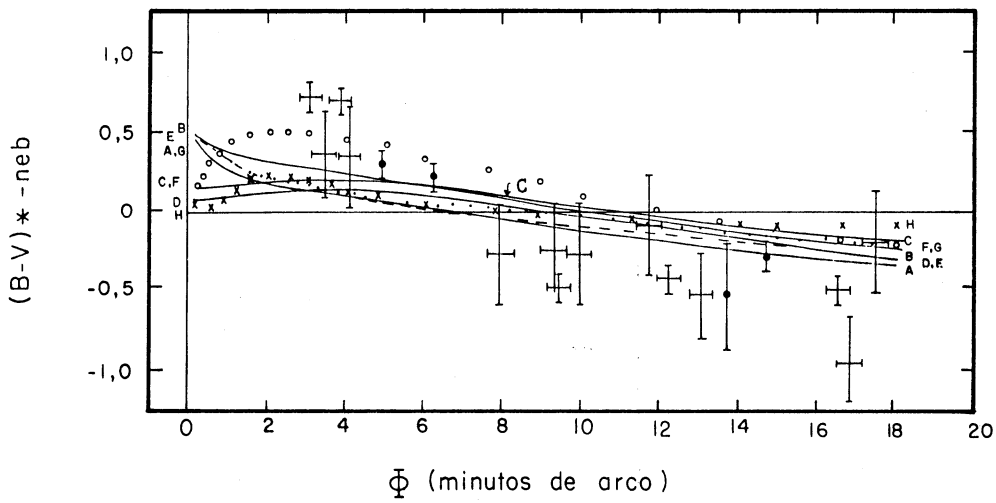

FIGURE 3. Models that reproduce the general trend of the observed $(B-V)_{*-neb}$ curves for all directions (see also Figures 4 and 5).

The only star-in-front model that was able to reproduce the observa-

© Universidad Nacional Autónoma de México • Provided by the NASA Astrophysics Data System

1986RMxAA..12..273D

tions is the one with ice (T= 0.1 pc and H= 0.1 pc).

(c) Star Inside

The most prominent feature of these models is the increasing similarity either to the star-behind predictions, as the star is progressively located deeper inside the slab, or to the star-in-front results, as the star approaches the surface.

For H= 0.1 pc and T varying from 1.0 pc to 1.5 pc, all materials show a reddening of no more than 0.1 mag. This might suggest that the results are not strongly affected when deeper layers are considered. For larger values of H this reddening also increases, pushing the upper limits for T to greater values. This might imply the existence of a definite value H/T < 1, which, for H < 1, would give the maximum T that still influences the results.

These were the models most successful in reproducing the $(B-V)_{*-neb}$ observed curves. The corresponding models in Figure 3 are:

- silica (T=2 and H=0.05; T=1.5 and H=0.1; T=1 and H=0.1)
- olivine (T=2 and H=0.05)
- ice (T=1.5 and H=0.9)
- dirty ice (k=-0.02, T=1 and H=0.9)
- dirty ice (k=-0.05, T=1.5 and H=0.9)

It can be seen in Figure 3 that these models reproduce the observed general behavior only, not being able to produce either the strong blue color near the star, or the steep transition to a red color, followed by a slow reddening away from the star. On the other hand, dirty ice (k=-0.05), olivine and silica adjust the blue part of the observed curve, for low values of T(Figure 4). Regions radially farther from the star could be fitted by ice, NH_3, magnetite and SiC (Figure 5)

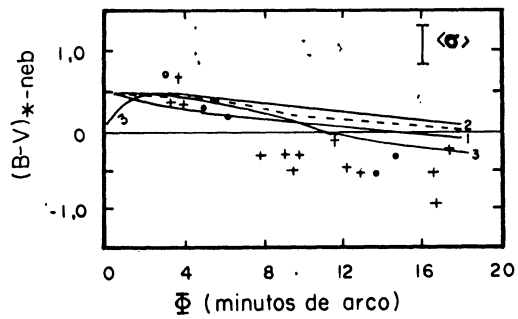

FIGURE 4. Models that adjust the blue part of the observed $(B-V)_{*-neb}$

© Universidad Nacional Autónoma de México • Provided by the NASA Astrophysics Data System

1986RMxAA..12..273D

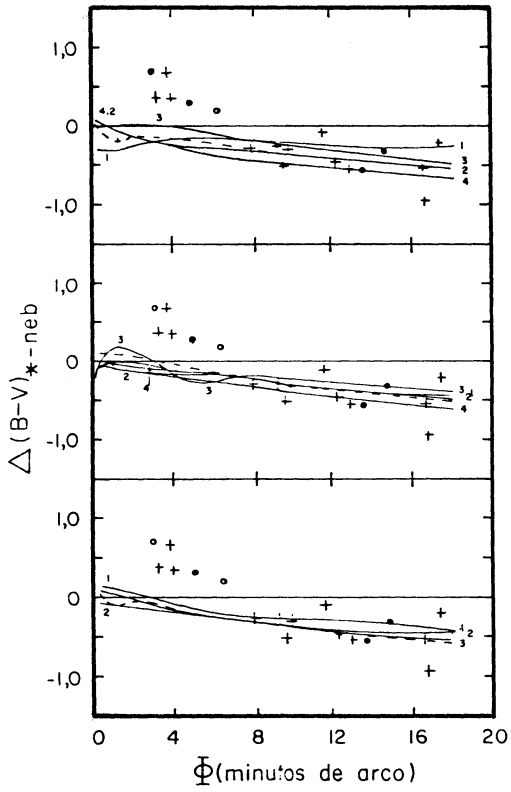

FIGURE 5. Models that give the best fits to the regions farther away from the star.

V. DISCUSSION AND CONCLUSIONS

Taking into account that ν Sco has a color excess E_{B-V}= 0.28 (Breger, 1976; Breakiron & Upgren, 1979; Abbott *et al.*, 1982), the application of this value in a distance-reddening relation with R= 3.2 (Pottasch *et al.*, 1977) would give too large a distance for this star, thus placing it out of the Sco-Cen association (Deutschman *et al.*, 1976).

Dahn(1967) suggested that this color excess, together with the nebula location in a rather obscure region of the sky, implies that the illuminating star is located either within or behind the nebula. No star-in-front models were able to fit all observations satisfactorily. On the other hand, all considered directions could be explained by a star-inside model with dirty ices , ice, silica and olivine and T≃ 1.5 pc and 0.05<H<0.5 pc. Ice and dirty ices require the star to be deeply embedded in the slab, but silica and olivine need just a tenuous dust layer in front of the illuminating star. The adopted color excess favors the star-inside model. Therefore we conclude that ν Sco is embedded in a tipical reflection nebula of ~1.5 pc, tilted 10^0 relative the plane of the sky; the stellar depth seems to be primarily a function of the grain

© Universidad Nacional Autónoma de México • Provided by the NASA Astrophysics Data System

1986RMxAA..12..273D

material employed.

More observational data is required for a better determination of either nebular models or dust grain chemical composition. Dirty ices, olivine, and silica are good candidates, but ice, NH_3, SiC and magnetite cannot however be excluded.

ACKNOWLEDGEMENTS

This work has received support from FAPESP, CAPES, CNPq and FINEP.

REFERENCES

Abbott, D.C., Bohlin, R.C., Savage, B.D. 1982, Ap. J. Suppl., 48, 369.
Breakiron, L.A., Upgren, A.R. 1979, Ap. J. Suppl., 41, 709.
Breger, M. 1976, Ap. J. Suppl., 32, 1.
Boggess, A., Borgman, J. 1964, Ap. J., 140, 1636.
Cameron, A.G.W. 1975 *in* "The Dusty Universe", eds. G.B. Field and A.G.W. Cameron, Neale Watson Acad. Publ., NY.
Dahn, C. 1967, Thesis, Case Institute of Technology.
Debye, P. 1909, Ann. Phys., 30, 59.
Deutschman, W.A., Davis, R.J., Schild, R.E. 1976, Ap. J. Suppl., 30, 97.
Greenberg, J.M. 1968, *in* "Nebulae and Interstellar Matter", eds. B. M. Middlehurst and L. H. Aller, Univ. of Chicago Press.
Hanner, M.S. 1969, Thesis, Rensselaer Ploytechnic Institute.
Hardie, R.H. 1962, *in* "Astronomical Techniques", ed. W.A. Hiltner, Univ. of Chicago Press, Illinois.
van de Hulst, H.C. 1957, "Light Scattering by Small Particles", John Wiley &Sons.
King, D.J., Scarrot, S.M., Taylor, K.N.R. 1983, M.N.R.A.S., 202, 1087.
Kurucz, R. 1979, Ap. J. Suppl., 40, 1.
Mie, G. 1908, Ann. Phys., 25, 377.
Oort, J.H., van de Hulst, H.C. 1946, B.A.N., 10, 187.
Roark, T.P. 1966, Thesis, Rensselaer Ploytechnic Institute.
Rossi, S.C.F., Maciel, W.J. 1984, Ap. Space Sci., 103, 143.
Schalén, C. 1945, Upp. Obs. Ann., 1, Nº 9.
Sellgren, K. 1984, Ap. J., 277, 623.
Shah, G.A., Krishna-Swamy, K.S. 1981, Ap. J., 243, 175.
Pottasch, S.R., Wesselius, P.R., Wu, C.-C., van Duinen,R.J. 1977, A. Ap., 54, 435.
Whittet, D.C.B. 1981, Q.J.R.A.S., 22, 3.
Zellner, B.H. 1970, Thesis, Univ. of Arizona.

M. de Oliveira and W.J. Maciel: Instituto Astronômico e Geofísico da Universidade de São Paulo, Caixa Postal 30.627, CEP 01051, São Paulo SP, Brasil.

© Universidad Nacional Autónoma de México • Provided by the NASA Astrophysics Data System